Viscoelasticity of randomly branched polymers in the vulcanization class

Charles P. Lusignan*
Department of Physics and Astronomy, University of Rochester, Rochester, New York 14627

Thomas H. Mourey
Imaging Research and Advanced Development-Materials, Eastman Kodak Company, Rochester, New York 14650-2136

John C. Wilson†
Office Imaging, Eastman Kodak Company, Rochester, New York 14650-2129

Ralph H. Colby
Department of Materials Science and Engineering, The Pennsylvania State University, University Park, Pennsylvania 16802

(Received 24 August 1998; revised manuscript received 11 June 1999)

We report viscosity, recoverable compliance, and molar mass distribution for a series of randomly branched polyester samples with long linear chain sections between branch points. Molecular structure characterization determines $\tau = 2.47 \pm 0.05$ for the exponent controlling the molar mass distribution, so this system belongs to the vulcanization (mean-field) universality class. Consequently, branched polymers of similar size strongly overlap and form interchain entanglements. The viscosity diverges at the gel point with an exponent $s = 6.1 \pm 0.3$, that is significantly larger than the value of 1.33 predicted by the branched polymer Rouse model (bead-spring model without entanglements). The recoverable compliance diverges at the percolation threshold with an exponent $t = 3.2 \pm 0.2$. This effect is consistent with the idea that each branched polymer of size equal to the correlation length stores $k_B T$ of elastic energy. Near the gel point, the complex shear modulus is a power law in frequency with an exponent $u = 0.33 \pm 0.05$. The measured rheological exponents confirm that the dynamic scaling law $u = t/(s+t)$ holds for the vulcanization class. Since s is larger and u is smaller than the Rouse values observed in systems that belong to the critical percolation universality class, we conclude that entanglements profoundly increase the longest relaxation time. Examination of the literature data reveals clear trends for the exponents s and u as functions of the chain length between branch points. These dependencies, qualitatively explained by hierarchical relaxation models, imply that the dynamic scaling observed in systems that belong to the vulcanization class is *nonuniversal*. [S1063-651X(99)12210-4]

PACS number(s): 61.41.+e, 82.70.Gg

INTRODUCTION

The evolution of molecular structure during random branching processes that ultimately leads to gelation is understood by percolation theory [1,2]. There are two universality classes for the gelation problem, separated by a Ginzburg criterion [3,4] that depends upon the chain length between branch points N [4,5] as well as the concentration of any nonreacting solvent [6]. In the absence of solvent, the vulcanization of long linear polymer chains (large N) belongs to the mean-field class and is modeled by Flory-Stockmayer theory [7–18]. Critical percolation (small N) describes the polymerization of small multifunctional monomers [1,19,20]. An experimental system with intermediate N will exhibit a crossover between mean-field behavior far from the gel point and critical behavior, close to the percolation threshold, in a manner similar to other continuous phase transitions.

In contrast to the molecular structure, the rheology of randomly branched polymers is not well understood. Our previous work [21,22] demonstrated that a molten polyester system with $N \cong 2$, prepared by polycondensation under conditions of unbalanced stoichiometry, belonged to the critical percolation universality class. A simple bead-spring model, with the usual Rouse approximation of no hydrodynamic or topological interactions, completely predicted the observed rheological properties. Indeed, this Rouse model was found adequate for systems with values of N as high as 20 [22–24].

In this paper we have prepared stable randomly branched polyesters, by reacting all the acid groups in an excess of hydroxyl groups, thereby halting the chemical reaction by stoichiometric imbalance. This approach allows us to determine the molar mass distribution and measure the terminal rheological properties, even near the gel point where the longest relaxation time is very large. We report structural and rheological data for a system with $N = 900$ (vulcanization class), demonstrating that topological interactions dominate the rheological response for systems with long linear chains between branch points. In particular, we find that the branched polymer Rouse model is not sufficient to describe the physics of these systems, and we suggest that entanglements must be accounted for to correctly predict the observed dynamic response.

*Author to whom correspondence should be addressed. Present address: Imaging Research and Advanced Development-Materials, Eastman Kodak Company, Rochester, NY 14650-2109.

†Present address: Heidelberg Digital, LLC, Rochester, NY 14650.

TABLE I. Static exponent values for percolation theory.

Exponent	Critical Percolation[a]	Vulcanization (mean-field)[b]	Defining Relation
τ	2.20 ± 0.05	$\frac{5}{2}$	(2)
σ	0.452 ± 0.011	$\frac{1}{2}$	(3)
γ	1.78 ± 0.09	1	(6)
ν	0.88 ± 0.02	$\frac{1}{2}$	(4)

[a]Calculated, at 95% confidence, by pooling the series and Monte Carlo data tabulated in Ref. [25].
[b]Exact values, from Ref. [1].

BACKGROUND THEORY

Two important parameters completely describe the state of any randomly branched polymer prepared by melt condensation: the relative extent of reaction ε and the average number of Kuhn monomers between branch points N. The relative extent of reaction is defined from the number of crosslinks formed, p, and the number required to reach the gel point p_c [1],

$$\varepsilon = \frac{|p_c - p|}{p_c}. \tag{1}$$

The degree of polymerization between branch points N is estimated from knowledge of the molecular structure obtained from size exclusion chromatography (SEC) experiments. Linear and branched structures have different swollen fractal dimensions, and exhibit different exponents on plots of intrinsic viscosity versus molar mass. We determine N from the intersection of these two power laws as described in the experimental section.

Static structure

We review briefly the molecular structure predictions of the percolation theory of gelation. The mean-field (vulcanization) and critical percolation classes have the same form for their scaling relations, but differ in their exponent values [1]. Static critical exponents for gelation are summarized in Table I.

The molar mass distribution of a gelling system is characterized by two scaling exponents τ and σ [1]. The number fraction of branched polymers $\Phi(M)$ of molar mass M is a power law in molar mass that is truncated at a characteristic molar mass M_{char} by an exponential cut-off function f:

$$\Phi(M) \sim M^{-\tau} f(M/M_{\text{char}}). \tag{2}$$

M_{char} diverges with exponent $1/\sigma$ as the gel point is approached,

$$M_{\text{char}} \sim \varepsilon^{-1/\sigma}. \tag{3}$$

The size of the largest branched polymer ξ is the correlation length for gelation and its divergence at the gel point defines another exponent ν through the power law [1],

$$\xi \sim \varepsilon^{-\nu}. \tag{4}$$

A number of measurable quantities are ratios of the moments of the molar mass distribution

$$M_q = \frac{\int \Phi(M) M^q dM}{\int \Phi(M) M^{q-1} dM}. \tag{5}$$

The ratio with $q=2$ yields the weight-average molar mass M_w, which diverges at the critical point as [1]

$$M_w \sim \varepsilon^{-\gamma}. \tag{6}$$

Higher order moment ratios, such as $q=3$ for the z-average molar mass M_z, are all proportional to the characteristic largest molar mass M_{char} [1,19].

Experimental determination of ε requires measuring the extent of reaction p and the critical extent of reaction at the gel point p_c. These measurements are made with a certain random error, thus, the relative uncertainty in ε diverges at the gel point [1,19]. We circumvent this problem by correlating two measurements with finite relative uncertainties. For example, using the scaling law

$$3 - \tau = \sigma\gamma, \tag{7}$$

we determine the exponent τ from a plot of M_{char} against M_w since

$$M_{\text{char}} \sim M_w^{1/\sigma\gamma} \sim M_w^{1/(3-\tau)}. \tag{8}$$

The exponent ν is related to the other static exponents in the critical percolation class through the hyperscaling relation [1,19,26]

$$3\nu = \frac{(\tau - 1)}{\sigma} \quad \text{(critical percolation)}. \tag{9}$$

In the mean-field limit, the Fisher law [1] plays a corresponding role,

$$\nu = \frac{\gamma}{2} = \frac{(3-\tau)}{2\sigma} \quad \text{(vulcanization)}. \tag{10}$$

Using similar scaling laws, all static exponents can be calculated from knowledge of any two, in either universality class. For vulcanization, the percolation model is exactly solvable, so we can write the cut-off function of Eq. (2) explicitly,

$$f_{\text{MF}}(M/M_{\text{char}}) = \exp[-M/(2M_{\text{char}})]. \tag{11}$$

The mathematical form of the cut-off function in the critical percolation class is unknown, because the three-dimensional critical percolation problem has only been solved numerically. Experimentally [21,22,27] and via Monte Carlo simulation [28–30] it has been established that the critical percolation cut-off function $f(M/M_{\text{char}})$ of Eq. (2) is approximated by a shifted Gaussian function (SG) of the form

$$f_{\text{SG}}(M/M_{\text{char}}) \approx \frac{\exp(-[z_{\max} - (M/M_{\text{char}})^{\sigma}]^2)}{\exp(-z_{\max}^2)}. \tag{12}$$

The parameter $z_{\max}=0.623$ depends only on the values of the critical exponents τ and σ and the mathematical form of Eq. (12). The calculation is presented in Appendix A of Ref. [22].

When dissolved in a solvent to form a dilute solution, the branched species may be separated according to their hydrodynamic size using SEC. In solution, the size R of a randomly branched polymer is related to its molar mass M by its swollen fractal dimension d_s [1,20];

$$R \sim M^{1/d_s}. \tag{13}$$

Intrinsic viscosity $[\eta]$ is the initial slope of a plot of viscosity as a function of polymer concentration. It is related to the radius of gyration, molar mass, and swollen fractal dimension through [20]

$$[\eta] \sim \frac{R^3}{M} \sim M^a, \tag{14}$$

with

$$a = \frac{3}{d_s} - 1. \tag{15}$$

Chain overlap and the Ginzburg criterion

The key concept necessary to understand both the static and the dynamic properties of randomly branched polymers is *chain overlap*. Daoud *et al.* [31] calculated the number of overlapping correlation volumes in the gel as the ratio of the gel fraction to the density of a single network strand (which spans the correlation volume). This concept is equivalent to the number n of overlapping randomly branched characteristic molecules of size ξ and molar mass M_{char}:

$$n \cong N^{1/2} \varepsilon^{-3\nu+(\tau-1)/\sigma}. \tag{16}$$

This result applies both above and below the gel point [22,32]:

In the critical percolation class $N=1$, and hyperscaling (9) requires that $(\tau-1)/\sigma=3\nu$ [1]. Thus, the number of overlapping characteristic molecules n is a constant of order unity. This result implies that the largest branched molecules in the system do not overlap with each other in the critical limit. Using this fact, and the self-similar structure of the branched polymers, it can be shown [1,32] that branched polymers of a given size do not overlap each other in the critical percolation class. The pervaded volume of a given randomly branched polymer in this limit is filled only with smaller molecules.

In the vulcanization class $N \gg 1$, and the hyperscaling relation does not apply since $(\tau-1)/\sigma > 3\nu$. Consequently, $n>1$ and multiple overlapping characteristic molecules span a correlation volume of size ξ. Prior to the commencement of the vulcanization reaction in a melt of long linear chains, there are $N^{1/2}$ other polymer chains that share the same pervaded volume of a given polymer coil [20]. As the reaction proceeds, the branched molecules grow—the largest ones overlapping each other to a lesser extent because the exponent of ε in Eq. (16) is positive. The Ginzburg point ε_G is the relative extent of reaction at which the largest polymers no longer overlap significantly. Here, the static structure of the system crosses from the mean-field class to the critical class [3,4]. Closer to the gel point ($\varepsilon < \varepsilon_G$) branched polymers continue to grow in such a way that they remain at the overlap threshold (with $N \cong 1$) [32].

At ε_G only one characteristic molecule spans a correlation volume and n reaches a value of unity. Solving Eq. (16) for the Ginzburg point (using mean-field exponent values) we recover the famous de Gennes formula [4]:

$$\varepsilon_G \sim N^{-1/3}. \tag{17}$$

Equation (17) implies that for large N, ε_G is quite small. Thus, the entire range of experimentally accessible ε will be in the vulcanization class and the studied branched polymers will be modeled by the Flory-Stockmayer theory [7–18]. We find that our $N=900$ system exhibits vulcanization class scaling in accord with these ideas. Further discussion of Eq. (17), and its implications, as well as recent computer simulation and experimental results supporting it can be found in [22].

Dynamic scaling and linear response

Theories predict [23,33–36] and experiment confirms [19,21–24,35,37–52] that in the vicinity of the liquid to solid transition, the rheological properties obey scaling laws. At the gel point, the shear relaxation modulus $G(t)$ is a power law in time. The complex shear modulus $G^*(\omega)$ and the complex viscosity $\eta^*(\omega)$ are power laws in frequency ω:

$$G(t) \sim t^{-u} \quad \text{and}$$

$$G^*(i\omega) = i\omega\eta^*(i\omega) \sim (i\omega)^u. \tag{18}$$

Below the gel point, the rheological properties exhibit power law scaling on time scales shorter than the longest relaxation time $\mathcal{T}$, beyond which the system follows the standard terminal response of a viscoelastic liquid [53]. $\mathcal{T}$ is the time it takes a characteristic molecule, of molar mass M_{char} and size ξ, to fully relax. In analogy with other continuous phase transitions [54] we define the dynamic exponent z through

$$\mathcal{T} \sim \xi^z \sim \varepsilon^{-\nu z}. \tag{19}$$

The viscosity η is the integral of the stress relaxation modulus [53]. The divergence of the viscosity at the gel point defines the dynamic critical exponent s,

$$\eta = \int_0^\infty G(t)dt \sim \int_0^{\mathcal{T}} t^{-u}dt \sim \mathcal{T}^{1-u}$$

$$\sim \varepsilon^{-\nu z(1-u)} \sim \varepsilon^{-s}, \tag{20}$$

where

$$s = \nu z(1-u). \tag{21}$$

The recoverable compliance J_e^o is related to the first moment of the stress relaxation modulus [53]. The divergence of the recoverable compliance at the gel point defines the dynamic critical exponent t,

$$J_e^o = \frac{1}{\eta^2}\int_0^\infty tG(t)dt$$

$$\sim \frac{1}{\eta^2}\int_0^{\mathcal{T}} t^{1-u}dt \sim \varepsilon^{2s}\mathcal{T}^{2-u}$$

$$\sim \varepsilon^{2s-\nu z(2-u)} \sim \varepsilon^{-t}, \tag{22}$$

with $t=\nu z(2-u)-2s$. Eliminating s using Eq. (21) determines

$$t = \nu z u. \tag{23}$$

Combining Eqs. (21) and (23) by eliminating the exponent combination νz yields the dynamic scaling law

$$u = \frac{t}{s+t}. \tag{24}$$

We demonstrated previously that Eq. (24) is valid for systems with $N=2$ [21,22] and $N=20$ [22,24] Kuhn segments between branch points; herein we confirm it for a system with $N=900$.

The relaxation time exponent νz in Eq. (19) can be expressed in terms of s and t by eliminating u in Eqs. (21) and (23),

$$\nu z = s+t. \tag{25}$$

Equation (25) is a manifestation of the linear viscoelastic relationship between the relaxation time and the terminal flow properties [53,55,56]:

$$\mathcal{T} = J_e^o \eta. \tag{26}$$

Beyond the gel point, the equilibrium modulus is understood to be proportional to k_BT per network strand because each branched polymer of size equal to the correlation length stores k_BT of elastic energy [24,57–59]. With n overlapping network strands in each correlation volume ξ^3, the network modulus beyond the gel point is

$$G_e \cong \frac{n}{\xi^3}k_BT \sim N^{-1}\varepsilon^{(\tau-1)/\sigma} \sim N^{-1}\varepsilon^t. \tag{27}$$

Thus, there is a simple scaling relation for the ''modulus exponent'' t that is valid in both static universality classes [24]:

$$t = \frac{\tau-1}{\sigma}, \tag{28}$$

so $t=2.65$ for critical percolation and $t=3$ for vulcanization. Both values have been observed experimentally [24,44,60]. Since Eq. (28) relates t directly to the static exponents describing the molar mass distribution, it is in essence a structural quantity itself. Eliminating t from Eq. (21) using Eqs. (24), (25), and (28) yields

$$s = \nu z - \frac{\tau-1}{\sigma}. \tag{29}$$

Equation (24) can be rewritten using Eqs. (25) and (28) to give

$$u = \frac{\tau-1}{\sigma\nu z}. \tag{30}$$

Thus, z is the only independent dynamic exponent for gelation. Furthermore, Eqs. (28)–(30) show that all the physics necessary to explain the rheology of branched polymer materials is contained in the molar mass distribution, the relaxation time, and the correlation length. The chain length between crosslinks N affects all three of these.

As discussed previously for statics, our inability to determine the gel point with sufficient precision precludes any meaningful calculation of the relative extent of reaction ε, so we evaluate exponent ratios by plotting measured quantities against each other. We make use of

$$\eta \sim M_w^{s/\gamma} \sim M_{\rm char}^{s\sigma} \tag{31}$$

for viscosity, and

$$J_e^o \sim M_w^{t/\gamma} \sim M_{\rm char}^{t\sigma} \tag{32}$$

for recoverable compliance, as well as

$$J_e^o \sim \eta^{t/s} \sim \eta^{u/(1-u)}. \tag{33}$$

An important test of dynamic scaling is to verify that the same relaxation exponent u is determined in the terminal zone from Eq. (33) and at higher frequencies from Eq. (18). We have previously verified this scaling for the critical percolation class (with $N=2$) [21,22], and in the crossover region (with $N=20$) [22,23] . In this paper we find that it also holds in the vulcanization class (with $N=900$).

EXPERIMENT

The molecular structure and rheology data discussed below are tabulated in Table II. The main results of this section are that the $N=900$ polyester system belongs to the vulcanization (mean-field) static universality class and that its rheology is not modeled by the branched polymer Rouse model. Entanglement effects should be prevalent in this system since $M_e=2100$ [61], which is of the same order as the molar mass of the precursor molecules.

Polyester synthesis

Hydroxy terminated polyesters with very low acid number were prepared from adipic acid (AD), trimethylolpropane (TMP), Terathane 2900 (DuPont)—a polytetramethylene glycol oligomer (PTMG) with $M_n=2900$—and Fascat 4100 (butyl stannoic acid) catalyst. Reactants were purchased from Aldrich Chemical Company and Eastman Chemical Company and used without further purification. The catalyst was purchased from M&T Chemicals and used without further purification.

The motivation for selecting this system was to produce stable branched polyesters with molecular structure in the vulcanization limit. Appropriate amounts of AD, TMP, and PTMG were determined using the ''Eastman Polyester Resin'' computer program (Eastman Chemical Company).

TABLE II. Molecular structure and rheology data. Entries indicated with a ‡ next to their M_w denote points appearing in Fig. 6.

M_w	$M_{\max}$	M_{char}	η (P)	J_e^0(cm^2/dyn)
12 300	27 000			
15 200‡	30 700	10 800	408	
18 900	36 700	17 200	832	
24 200‡	47 300	20 400	2020	
27 900‡	56 900	45 500	4180	0.000 009 20
37 500‡	76 600	77 000	11 600	0.000 0175
45 300	99 000	135 000	27 000	0.000 0320
53 400‡	129 000	172 000	51 200	0.000 0428
58 300	144 000	187 000		
68 300‡	174 000	282 000	358 000	0.000 0873
85 300‡	222 000	422 000	524 000	0.000 144
145 000‡	587 000	1020 000	39 800 000	0.001 33
226 000‡	1190 000			

Entering arguments were a PTMG:TMP molar ratio of 3:1, an acid number of zero. For each target number average molar mass, the computer program calculated the reactant quantities to use. The reactants were then weighed and a yield of 250 g of polymer. into a triple neck 500-ml round-bottom flask along with 0.25 g of Fascat 4100. The AD concentration was adjusted to produce a series of randomly crosslinked end products at the specified molar masses. The flask was fitted with a Teflon blade stirrer, Teflon bearing, nitrogen inlet, and a steam heated partial condensing packed column with a water cooled distillation head and receiver. The flask was then immersed in a 200 °C salt bath and continuously stirred from 1.75 to 3.75 h, collecting the water distillate formed. The bath temperature was then increased to 220 °C and stirring was continued for 24–31 h. At this stage, the branched polymer was stirred under water aspirator vacuum for approximately 0.5 h, then poured from the flask into amber storage jars and cooled to room temperature. Samples were stored under dry nitrogen to minimize the absorption of water. All samples had acid numbers of 0.017 meq/g or less as determined by nonaqueous titration. This demonstrates the complete reaction of all the acid groups.

Sample preparation for the four highest molar mass samples was slightly different. These samples were partially reacted for 4 h in a 500-ml flask at 200 °C while being continuously stirred. The samples were then poured into small aluminum dishes and reacted under nitrogen at 220 °C for 48 h. Acid numbers near zero again demonstrated complete chemical conversion of the acid groups.

Size exclusion chromatography

Using SEC each sample was separated into fractions containing molecules of roughly the same hydrodynamic size. These fractions were subsequently passed through three detectors placed in series after the SEC columns: two-angle laser light scattering (TALLS), differential refractive index (DRI), and viscometry. Used together, these detectors can determine the molar mass, concentration, and intrinsic viscosity of each eluted fraction. The method is discussed in [21,62,63] and references therein. The PTMG polyester has a specific refractive index increment $dn/dc = 0.0640$ ml/g at 680 nm in THF. The eluent was uninhibited tetrahydrofuran (THF). All samples were prefiltered through 0.2-μm Anatop inorganic membranes and injected in 100 μL amounts. No filters were inserted between the columns and the detectors. The effective interdetector volume between the TALLS and DRI detectors was determined using the systematic approach described in [62]. The column set used consisted of three 7.5-mm-diameter×300-mm-long Polymer Laboratories mixed-*C* PL gel columns. The nominal flow rate was 1.0 ml/min with sample concentrations in the range 2.0 mg/ml (highest molar masses) to 6.0 mg/ml (lowest molar masses). Acetone (0.2%) was used as an internal flow marker.

Figure 1 is a plot of the intrinsic viscosity, as a function of weight-average molar mass, combining SEC fractions from all the samples in this study. Two power laws are evident—see Eqs. (14) and (15)—and their intersection at a molar mass of $M_x = 66\,000$ indicates the typical linear chain molecular weight in the system. Fractions of the distribution with $1.2\times10^4 < M < 4\times10^4$ have slope $a = 0.803 \pm 0.021$, corresponding to a swollen fractal dimension of $d_s = 1.66 \pm 0.02$. The known linear chain value is $\frac{5}{3}$ [20], so these results indicate that linear chains dominate the low molecular weight region of the distribution. Fractions with $2\times10^5 < M < 8\times10^5$ have slope $a = 0.449 \pm 0.016$, corresponding to a swollen fractal dimension of the branched chains of $d_s = 2.07 \pm 0.02$. Thus the intersection of the two power laws in Fig. 1, at $M = M_x$, determines the crossover point between branched and linear behavior. M_x is a measure of the average molar mass between crosslinks. Since the PTMG repeat unit (molar mass $M_0 = 72$) is the same as its Kuhn segment [61], we calculate $N = M_x/M_0 = 900$. This value is much larger than the degree of polymerization of the linear PTMG precursor molecules ($DP = 40$). The linear chain between branch points consists of roughly 23 PTMG oligomers. For an ideal 3:1 PTMG:TMP reaction we except 3 PTMG molecules per chain. Thus, the reactivity of the third OH group on the TMP is roughly eight times slower than the reactivity of the other two OH groups.

Weight-average molar mass of each sample M_w determined by integration of the low-angle light scattering detector signal (without the DRI) as described in [21,62,63], is

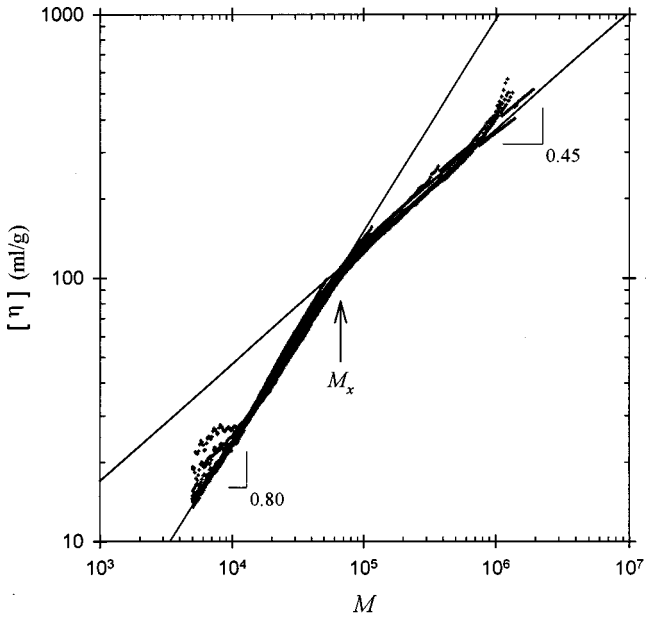

FIG. 1. Intrinsic viscosity as a function of the molar mass from SEC. The solid line with slope 0.45 ± 0.02 corresponds to a randomly branched polymer. The solid line with slope 0.80 ± 0.02 corresponds to a linear polymer. The arrow indicates the crossover from branched to linear at $M_x = 6.6 \times 10^4$, which determines $N = 900$.

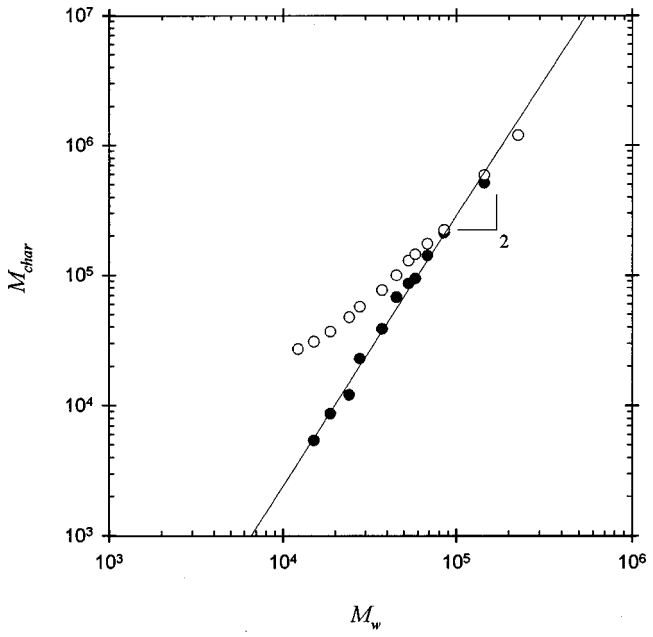

FIG. 2. Two measures of the largest characteristic molar mass correlated with the weight-average molecular weight. Open circles are $M_{\max}$ determined from light scattering as described in the text. Filled circles are M_{char} (divided by two to superimpose the data at high molecular weight) determined by fitting the molar mass distribution to the Flory-Stockmayer theory, as shown in Fig. 3. The line indicates a slope of 2, corresponding to $\tau = \frac{5}{2}$ [see Eq. (8)].

listed in Table II. Also tabulated is $M_{\max}$, the peak at the elution volume corresponding to the maximum scattered intensity. Table II also presents M_{char} determined from the molecular weight distribution using the fitting procedure discussed below. Previous gelation studies demonstrated that $M_{\max} \propto M_z \propto M_{\text{char}}$ [21,22,27,64–66]. Typical uncertainties in molecular weight, averaging 6 to 8 replicate analyses, are $\pm 10\%$ in M_w; $\pm 12\%$ in $M_{\max}$; and $\pm 20\%$ in M_z.

Assuming that each elution volume V_i corresponds to a single molar mass, the number of molecules $\Phi(M_i)$ of molecular weight M_i is given by [22,62,63]

$$\Phi(M_i) = -\frac{N_A}{2.303(M_i)^2}\frac{c_i}{c}\frac{dV_i}{d\log(M_i)}, \tag{34}$$

where c is the area under the DRI chromatogram, and c_i/c is the weight fraction of polymer in the ith retention volume V_i, and the derivative is obtained from the standard SEC [$\log(M)$ vs V] calibration curve.

Two measures of the characteristic largest molecular weight, $M_{\max}$ and M_{char} are plotted against M_w in Fig. 2. The expected power law correlation (8) fails for $M_{\max}$ vs M_w at low molecular weights ($M_w < 10^5$) because the $M_{\max}$ peak is dominated by the signal from the linear chains. Closer to the gel point, the data are consistent with static scaling expectations: $M_{\max} \propto M_{\text{char}}$. Judging from the figure, the effect of linear chains persists up to $M_{\text{char}} \cong 2M_x$.

Scaling theory predicts that the correlation length ξ is the only relevant length scale in the gelation problem near the gel point [1,19]. Hence, M_{char} is the only relevant molar mass scale. $M_x = 6.6 \times 10^4$ represents the lower bound in M_{char} where percolation/gelation ideas can be applied. Molecules with molar mass smaller than this are mostly linear polymer chains.

For linear polymers, one expects $M_{\max} \propto M_w$, and indeed we find that

$$\frac{M_{\max}}{M_w} = 2.03 \pm 0.11 (95\%) \quad M_{\max} < M_x. \tag{35}$$

To determine the static universality class for the system, $\Phi(M)$ was calculated by Eq. (34) for each sample. These data were then fit to the product of a power law and an exponential cut-off function. Data corresponding to $M_{\max} < 2M_x$ were removed from the distribution so that just the effects of the random branching could be studied. The τ value was not immediately obvious from the shape of the molar mass distribution for the samples closest to the gel point because the cut-off function interfers with the power law slope. Fitting the $\Phi(M)$ data first to Eq. (2) with $\tau = \frac{5}{2}$ and the vulcanization cut-off function given by Eq. (11), and second to Eq. (2) with $\tau = 2.2$ and the critical percolation cut-off function given by Eq. (12) with $z_{\max} = 0.632$, produced equally good results, as demonstrated in Fig. 3. This spurious result is due to the limited range covered by the molar mass distribution that corresponds to branched polymers. The fitted M_{char} values from both fits are plotted in Fig. 4 as functions of weight-average molar mass. The M_{char} values from the vulcanization class fit, with $\tau = \frac{5}{2}$ are presented in Table II. Linear regression of these points in Fig. 4 determines $1/(3-\tau) = 1.87 \pm 0.19$, thus

$$\tau = 2.47 \pm 0.05 \ (95\%), \tag{36}$$

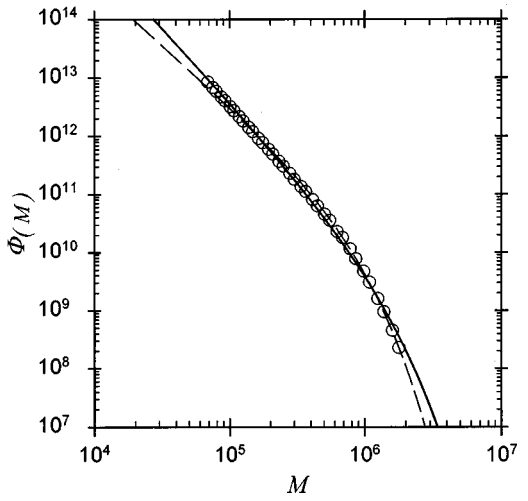

FIG. 3. Experimentally determined molar mass distribution (every tenth point) for the sample with $M_w = 8.53 \times 10^4$. Curves are two-parameter fits to the two possible forms of the distribution function: the critical percolation limit (dashed curve) using $\tau = 2.2$ with Eqs. (2) and (12), and the vulcanization limit (solid curve) using $\tau = \frac{5}{2}$ with Eqs. (2) and (11).

for the $N = 900$ system. The parallel slopes of M_{char} values obtained from the critical percolation and vulcanization models of the distribution, shown in Fig. 4, demonstrate that $\tau \cong \frac{5}{2}$ for this system regardless of which fit was used. Thus the choice of $\tau = 2.2$ in the critical percolation fit is inconsistent. Therefore, the molecular structure of the $N = 900$ randomly branched polyesters places them in the vulcanization universality class.

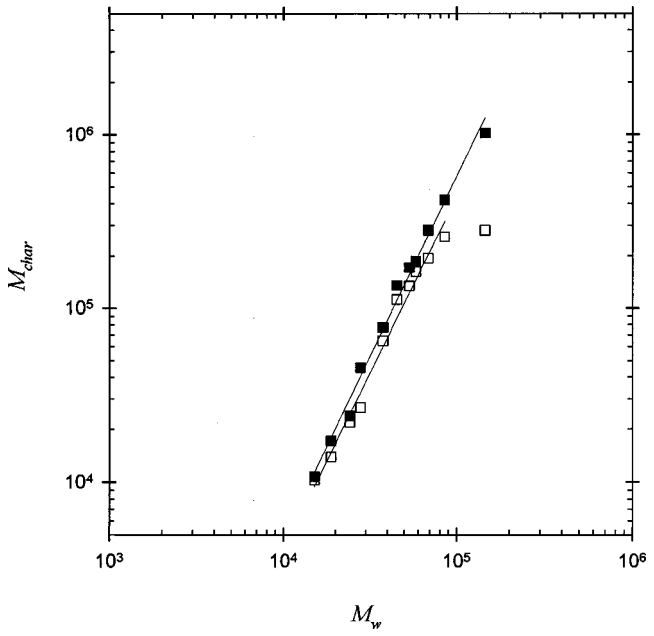

FIG. 4. Correlation of the characteristic largest molar mass with the weight-average molar mass. Each SEC data set was fit to both mean-field distribution (filled symbols): $\tau = \frac{5}{2}$ with Eqs. (2) and (11); and the critical percolation distribution (open symbols): $\tau = 2.2$ with Eqs. (2) and (12). Regression of the mean-field fitted points determines $\tau = 2.47 \pm 0.05$. Since the regression line through the critical fitted points (with the exception of the last) is parallel to the mean-field fitted ones, the choice of $\tau = 2.2$ is inconsistent. Therefore, this system belongs to the vulcanization universality class.

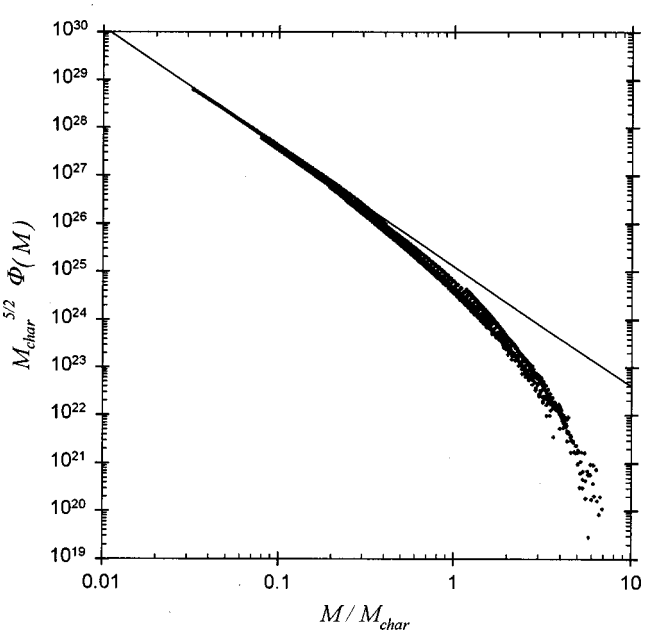

FIG. 5. Universal molar mass distribution constructed from Eq. (37). Molar masses smaller than $2M_x$ were removed from each curve prior to shifting. The solid line is a power law with slope of $-\frac{5}{2}$. The excellent data collapse refers to Eq. (37) in this plot demonstrates that this system with $N = 900$ is in the vulcanization universality class.

The molar mass distribution master curve, Fig. 5, is the final proof that this system belongs to the vulcanization universality class. The master curve is constructed from the experimental $\Phi(M)$ for all the samples with $M_x > 6.6 \times 10^4$ and the fitted M_{char} data for $\tau = \frac{5}{2}$ according to the equation

$$M_{\text{char}}{}^{5/2}\Phi(M) \propto (M/M_{\text{char}})^{-5/2} \exp[-M/(2M_{\text{char}})]. \qquad (37)$$

Attempts to construct similar master curves using $\tau = 2.2$ and the SG cut-off function (12) failed [22].

Oscillatory shear

Small-amplitude oscillatory strain response was measured using a Rheometrics System Four rheometer with 25-mm-diameter parallel plates. Standard linear viscoelasticity procedures [53] were employed as detailed in [22]. Since this polymer has a melting transition at about 22 °C, samples were molded under weak vacuum (about 0.2 atm) at approximately 70 °C under a 10-lb compressional load. After several days, the heat was removed and the sample allowed to recrystallize for several more days. It could then be easily removed from the mold and inserted in the rheometer and heated to 60 °C for testing in the liquid state. Frequency sweeps from 0.001 to 100 rad/s were made at 60 °C. DSC experiments revealed that the system's glass transition temperature remains constant at $T_g = -74.1 \pm 1.5$ °C across the entire range of samples studied.

The frequency dependence of complex viscosity is plotted in Fig. 6, for eight representative samples. Although too massive for accurate SEC determination of M_{max}, the vis-

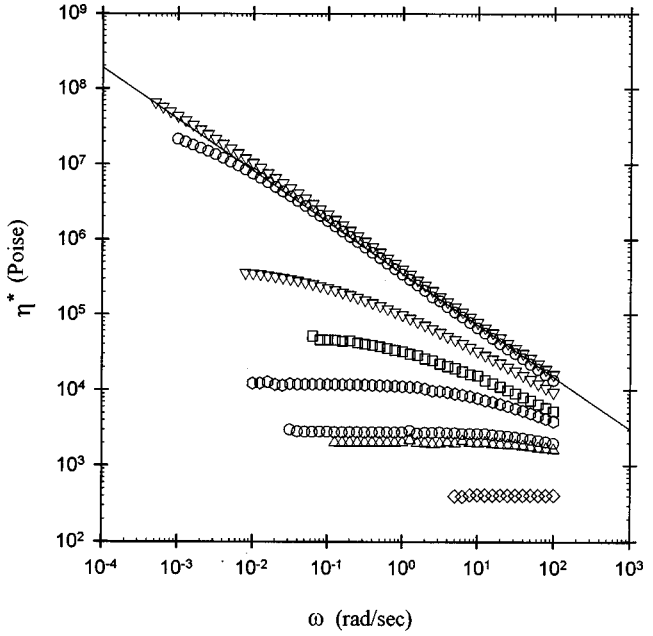

FIG. 6. Frequency dependence of the complex viscosity at 60 °C, for samples of increasing molar mass (moving vertically). The line is the simultaneous regression, over the frequency range 10–100 rad/s, to a power law with exponent $1-u$, for the $M_w=2.26\times10^5$ (triangles) and $M_w=1.45\times10^5$ (circles) samples. Regression to both, in the frequency region indicated in Fig. 7, yields $u=0.31\pm0.02$.

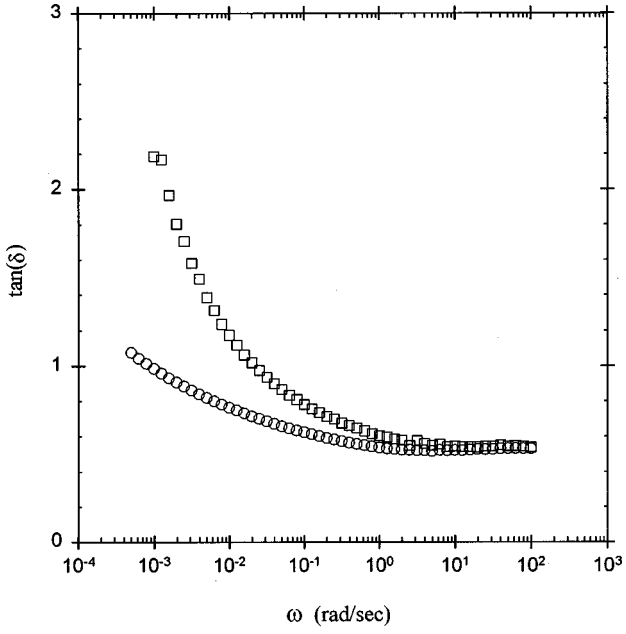

FIG. 7. Determination of the exponent $u=0.31\pm0.02$ from the two samples closest to the gel point: $M_w=2.26\times10^5$ (circles) and $M_w=1.45\times10^5$ (squares). Only data in the frequency range between 10 and 100 rad/s corresponds to pure gelation scaling (no interference with the crossover to terminal flow). In this frequency range the phase angle δ is related to u through the relationship $u=2\delta/\pi$.

coelastic response of the sample with $M_w=2.26\times10^5$ was also probed. Only the two samples closest to the gel point appear to have an obvious power law in the frequency dependence of complex viscosity that is independent of extent of reaction at high frequencies. Figure 7 demonstrates that, for the two samples with the highest molecular weight, frequencies between $10<\omega<100$ rad/s correspond to the pure power law region where $\tan\delta=G''/G'$ is independent of the probe frequency ω. Using the loss tangent we can calculate the relaxation exponent from the expression $u=2\delta/\pi$ [36,50,51]. Regression using data from both samples in this region yields $\tan\delta=0.53\pm0.04$, so that $u=0.31\pm0.02$. The frequency dependence of complex viscosity in Fig. 6 shows the same value of u,

$$u=0.31\pm0.02\ \ (95\%). \tag{38}$$

Creep and recovery

The terminal response near the gel point cannot be determined in the oscillatory strain experiment because the relaxation times become too long (see Fig. 6). A computerized version of Plazek's magnetic bearing torsional creep rheometer [67] was used to measure creep and subsequent recovery. Samples were molded in the same manner as for the oscillatory strain tests. Characterization was performed in the 16-mm-diameter parallel plate geometry under nitrogen atmosphere at a constant temperature of 60.0 ± 0.5 °C. The procedures are detailed in [22]. Samples close to the gel point required shear rates on the order of $5\times10^{-5}\,s^{-1}$ to achieve zero shear rate response. Creep times of approximately 10^5 s were necessary to achieve steady state for the samples closest to the gel point. Multiple determinations were made.

At long times in creep the strain varies linearly with time and the viscosity is calculated as the ratio of applied stress

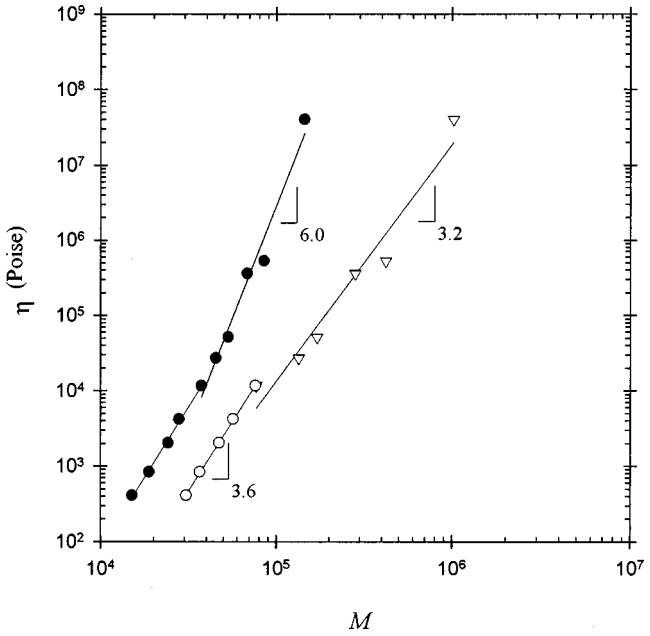

FIG. 8. Viscosity at 60 °C as functions of weight-average molar mass M_w (filled circles), characteristic largest molar mass $M_{\rm char}$ (open triangles), and the molar mass corresponding to the maximum light scattering $M_{\rm max}$ (open circles). Lines are regression to power laws with the indicated slopes.

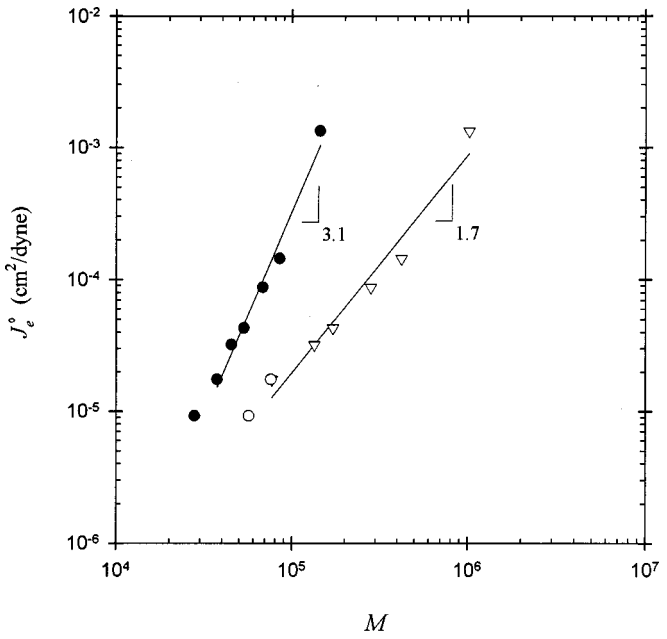

FIG. 9. Recoverable compliance at 60 °C as functions of weight-average molar mass M_w (filled circles), characteristic largest molar mass M_{char} (open triangles), and the molar mass corresponding to the maximum light scattering M_{max} (open circles). Lines are regression to power laws with the indicated slopes.

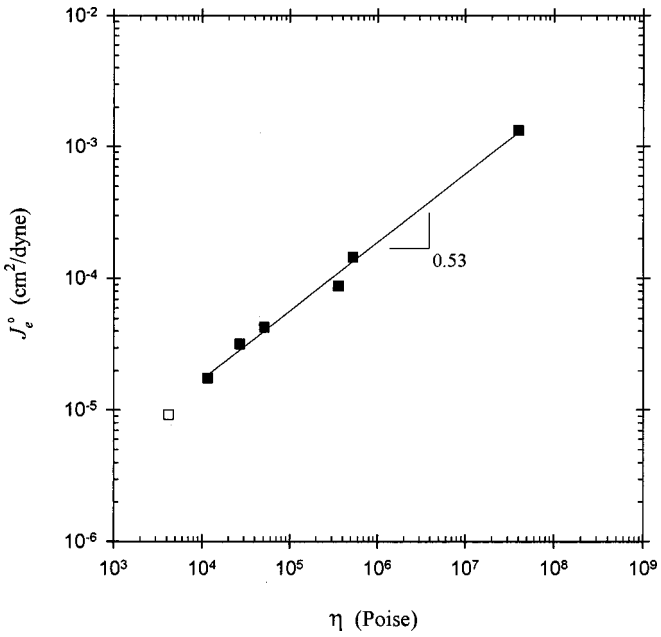

FIG. 10. Correlation of recoverable compliance with viscosity at 60 °C. The slope of the linear regression is $t/s=0.53\pm0.02$, thus $u=0.35\pm0.01$. The data point in the linear chain region (open square) with $M_{\mathrm{char}}<M_x$ was not included in the regression analysis.

and measured shear rate. Viscosity data are listed in Table II and are plotted in Fig. 8 as functions of molar mass. Two distinct regions of power law behavior corresponding to linear and branched rheological response are apparent, with the same crossover point as observed for intrinsic viscosity in Fig. 1. A previous study of randomly end-linked polydimethyl siloxane (PDMS) obtained similar results [45].

Samples with $M_{\mathrm{char}}<M_x=6.6\times10^4$, which corresponds to $M_w<3.5\times10^4$, are primarily comprised of linear polymer chains. Fitting the viscosity data to a power law in M_w, we find that these chains are entangled, since

$$\eta\propto M_w^{3.6\pm0.2},\quad M_{\mathrm{char}}<M_x=6.6\times10^4, \tag{39}$$

consistent with experimental results on entangled linear polymers [53,56]. The same is obviously true for η as a function of M_{max} in this regime. Samples with $M_w>3.5\times10^4$ correspond to branched polymers and have the exponent ratios

$$s/\gamma=6.0\pm0.5\ \ (95\%)\ \ \text{from}\,M_w,\ \text{and}$$

$$s\sigma=3.2\pm0.3\ \ (95\%)\ \ \text{from}\,M_{\mathrm{char}}. \tag{40}$$

Combining Eq. (40) with the mean-field exponents $\gamma=1$ and $\sigma=\frac{1}{2}$ from Table I leads to two estimates for s, which we pool to obtain

$$s=6.1\pm0.4\ \ (95\%). \tag{41}$$

After reaching steady state in creep the stress is removed and the angular elastic recoil (recoverable strain) is measured. The total recoverable strain divided by the initial applied stress is the recoverable compliance J_e^o. Recoverable compliance data are listed in Table II and plotted against M_w and M_{char} in Fig. 9. Few points in the linear chain regime are available because inertia interferes with the recovery measurement if the viscosity is less than about 10^4 P. Again, samples with $M_w>3.5\times10^4$ correspond to branched polymers and have the exponent ratios

$$t/\gamma=3.1\pm0.2\ \ (95\%)\ \ \text{from}\,M_w,\ \text{and}$$

$$t\sigma=1.7\pm0.2\ \ (95\%)\ \ \text{from}\,M_{\mathrm{char}}. \tag{42}$$

Combining Eq. (42) with the mean-field exponents $\gamma=1$ and $\sigma=\frac{1}{2}$ from Table I leads to two estimates for t, which we pool to establish that

$$t=3.2\pm0.2\ \ (95\%). \tag{43}$$

Finally, recoverable compliance is plotted against viscosity in Fig. 10, yielding a slope $t/s=0.53\pm0.02$. This ratio provides another measure of $u=(t/s)/[1+(t/s)]=0.35\pm0.01$ (95%) in reasonable agreement with the value of $u=0.31\pm0.02$ obtained in the oscillatory strain experiments at intermediate frequencies. We take this as evidence that Eq. (24) is valid and pool the two measures to obtain our best estimate for the relaxation exponent

$$u=0.33\pm0.05\ \ (95\%). \tag{44}$$

DISCUSSION

We previously studied a system with $N=2$, and found that it belonged to the critical percolation universality class [21,22]. A simple Rouse-type bead-spring model, that neglects interactions between chains, adequately described the linear viscoelasticity of this system [21–23,59,68]. Even though the molecular weight of the largest branched polymers becomes quite large (of order 10^7), they do not en-

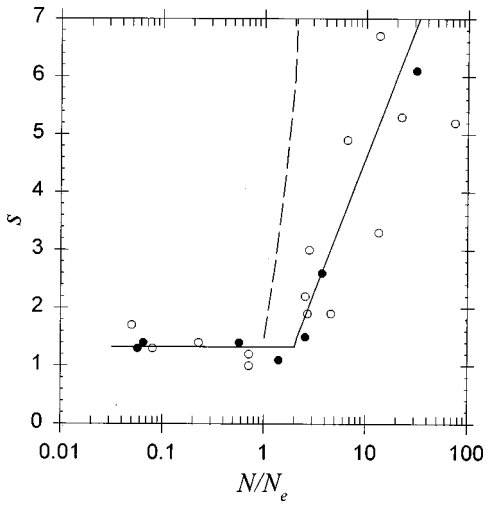

FIG. 11. Variation of the viscosity exponent s with the number of entanglements N/N_e between branch points for the data summarized in Table III. The solid symbols indicate systems where both the molecular structure and the rheology were determined. The open symbols are for systems where either s or M_x is estimated as indicated in Table III. The solid line is the Rouse model prediction of $s=1.33$ for $N/N_e<2$; and Eq. (46), a phenomenological form to account for entanglement effects, for $N/N_e>2$. The dashed line is calculated from Eq. (45) assuming $u=t/(s+t)$ with $t=3$.

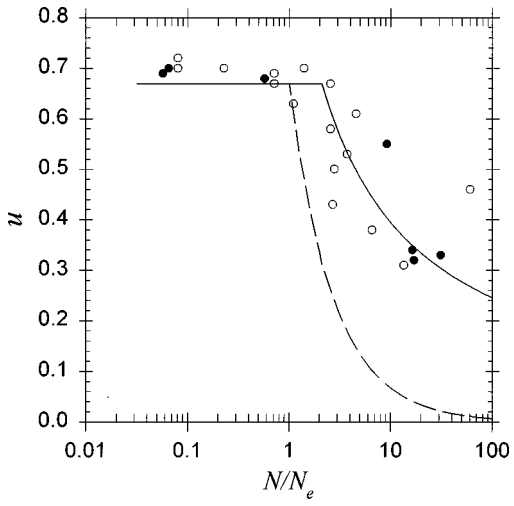

FIG. 12. Variation of the relaxation exponent u with the number of entanglements N/N_e between branch points for the data summarized in Table III. The solid symbols indicate systems where both the molecular structure and the rheology were determined. The open symbols are for systems where either u or M_x is estimated as indicated in Table III. The solid line is the Rouse model prediction of $u=0.67$ for $N/N_e<2$; and Eq. (47), a phenomenological form to account for entanglement effects, for $N/N_e>2$. The dashed line is Eq. (45), the prediction of the hierarchical relaxation model of [69].

tangle because hyperscaling permits them to overlap only with smaller branched polymers ($n\cong 1$). However, the $N=900$ system is in the mean-field limit where significant molecular overlap occurs ($n\gg 1$), so that for this system entanglements control the dynamics. This effect is most clearly evident through examination of the values for the relaxation time exponent νz as a function of N. The Rouse model predicts $\nu z=4.0$, and our previous work determined $\nu z=4.1$ for both the $N=2$ [21,22] and $N=20$ [22,24] systems. *However, in the present* $N=900$ *system we find* $\nu z=9.3$.

Figures 11 and 12, as well as Table III, demonstrate how the dynamic scaling exponents change as the number of entanglements between branch points N/N_e increases. N_e is the number of Kuhn monomers in an entanglement strand, and this ratio is identical to M_x/M_e—the ratio of the molecular weight between branch points to the entanglement molecular weight. In the figures, we present data from systems in which both the statics and dynamics were characterized simultaneously (filled symbols), and also systems where the dynamic response was measured and the static structure can be inferred from existing data (open symbols). It is clear that the branched polymer Rouse model predicts the observed dynamic response for $N/N_e<2$. Systems with longer linear chain sections between branch points systematically deviate from the Rouse predictions, presumably indicating the importance of interchain entanglements.

A theory of the entangled relaxation of branched polymers in the vulcanization class has been formulated for a system right at the gel point [69]. This model predicts that u is a function of N/N_e,

$$u=\psi\frac{N_e}{N} \quad \text{for } N\geqslant N_e, \tag{45}$$

where ψ is a constant. We take $\psi=0.67$ as in [69] and plot Eq. (45) as the dashed line in Fig. 12. The dashed line in Fig. 11 is predicted using u calculated from Eq. (45) and the equation $s=t(1-u)/u$ with $t=3$. It is clear from these figures that, while this theory qualitatively predicts the correct trend of u decreasing with increasing N/N_e, the quantitative comparison is quite poor.

Without a proper theory, we turn to a phenomenological description to model the N dependence of the rheological exponents observed in systems that belong to the vulcanization class. Figures 11 and 12 suggest that the Rouse model holds for $N/N_e<2$. For entangled linear polymer systems, the viscosity exhibits the effects of the entanglements at values typically 2 to 3 times larger than N_e [53]. It has also been observed that entanglement effects in randomly branched systems occur at larger values of N than in linear systems [45]. For example, randomly branched PDMS has $M_e=1.0\times 10^4$ [53], its linear chain entanglement crossover occurs at $M_c\cong 3.0\times 10^4$ [45,53], but the branched polymer entanglement crossover is at $M_c\cong 1.0\times 10^5$ [45]. Since there is only one independent dynamical exponent, the data in Figs. 11 and 12 must cross between Rouse and entangled dynamics at a single value of $N/N_e\cong 2$. The empirical functions are

$$s=\begin{cases}1.33 & N<2N_e\\ 2\ln(N/N_e) & N>2N_e,\end{cases} \tag{46}$$

and

$$u=\frac{t}{s+t}=\begin{cases}0.67 & N<2N_e\\ \dfrac{3}{3+2\ln(N/N_e)} & N>2N_e.\end{cases} \tag{47}$$

TABLE III. Dependence of the scaling exponents on N/N_e. Unless otherwise noted, M_x was taken to be the precursor chain molecular weight. Values of M_e used to calculate $N/N_e = M_x/M_e$ were obtained from [61]. In cases where γ was not measured directly the values are inferred from the static structure: $\gamma=18$ for $\tau=2.2$, $\gamma=1.4$ for $\tau=$-2.3, $\gamma=1.2$ for $\tau=2.4$, and $\gamma=1$ for $N/N_e > 2$ where $\tau=2.5$.

N/N_e	τ	γ	s/γ	s	u	Ref.
0.06	2.2	1.8	0.76	1.3	0.69	[21,22]
0.06		1.8	0.82	1.4	0.70	[38,40]
0.06		1.8	0.98	1.7[a]		[70]
0.08				1.3	0.70	[75]
0.08					0.72	[76]
0.23		1.4	1.0	1.4[a]	0.70[b]	[71,72]
0.57	2.3	1.4	1.1	1.4[c]	0.68	[22,66]
0.71				1.0	0.67	[43]
0.71				1.2	0.69	[73]
1.1					0.63	[74]
1.4	2.4	1.2	0.94	1.1[a]	0.73[b]	[22]
2.6[d]		1	1.5	1.5[a]	0.67[e]	[45]
2.6		1		2.2[c]	0.58	[46–48,50]
2.7		1		1.9	0.43	[43]
2.8		1		3.0[e]	0.5	[46–48,50]
3.7[d]		1	2.6	2.6[a]	0.53[b]	[45]
4.6		1		1.9[e]	0.61	[80,81]
6.6		1		4.9[e]	0.38	[80,81]
9.2[f]		1			0.55	[78]
13		1	3.3	3.3[a]		[77]
13		1		6.7[e]	0.31	[80,81]
16[f]		1			0.34	[78]
17[f]		1			0.32	[78]
22		1	5.3	5.3[a]		[79]
31	2.5	1	6.0	6.1	0.33	This work, [22]
60[g]		1			0.46	[82]
74		1	5.2	5.2[a]		[83]

[a]Estimated from measured s/γ using the γ values indicated in the table. In cases where γ was not measured directly, the values are inferred from the static structure: $\gamma=1.8$ for $\tau=2.2$, $\gamma=1.4$ for $\tau=2.3$, $\gamma=1.2$ for $\tau=2.4$, and $\gamma=1$ for $N/N_e>2$ where $\tau=2.5$.

[b]Estimated u from s and t using $u=t/(s+t)$ with the values $t=3$ for $N/N_e>2$, and $t=2.67$ for $N/N_e<2$.

[c]Estimated s from the measured $s\sigma$ and s/γ using the effective crossover values $\sigma=0.48$ and $\gamma=1.4$.

[d]M_x estimated using the g-factor and M_c from [45] via $M_x = gM_c$.

[e]Estimated $s=(t(1-u)/u)$ using $t=3$ and the measured u. $\sigma = 0.48$ and $\gamma=1.4$.

[f]M_x calculated from the measured (SEC) number of monomers between branch points P_{Napp} in [78].

[g]M_x chosen as the branched to linear crossover from the (SEC) data in [82]. The value $M_e=830$ was used [61]. However, M_e for polyethylene is controversial, with values reported in the literature in the range 830 to 2100.

Equations (46) and (47) model the data quite well and are shown as the solid curves in Figs. 11 and 12. The two expressions are chosen to go through the points where M_x was measured experimentally (filled symbols). The scatter of the data where M_x was estimated (open symbols) about the lines is probably due to errors in our estimation procedure, in which M_x was taken to be the precursor chain length unless other information was available (see footnotes in Table III). In these cases, M_x, and thus N/N_e, may have significant error. In all cases, values of M_e were obtained from [61].

CONCLUSIONS

We measured the molar mass distribution of a series of randomly branched polyesters with long linear chain sections between branch points. We find that the mean-field Flory-Stockmayer theory adequately models the molecular structure of this system. We measured an exponent $\tau=2.47 \pm 0.05$, consistent with this system belonging to the vulcanization universality class, whose signature is $\tau=\frac{5}{2}$. Comparison of the intrinsic viscosity and molar mass fractions separated by size exclusion chromatography determines the number of Kuhn monomers between branch points to be $N = 900$.

From torsional creep and recovery experiments, we determined the viscosity and modulus exponents $s=6.1\pm0.4$ and $t=3.2\pm0.2$ below the gel point. The stress relaxation exponent determined by oscillatory shear agrees well with the corresponding value determined from the terminal response in the creep/recovery experiment. The pooled result is $u = 0.33\pm0.05$. These data verify that the dynamic scaling law $u=t/(s+t)$ applies in the vulcanization limit. The modulus exponent t is consistent with the idea that k_BT of elastic energy is stored per characteristic molecule. The observations, that the viscosity exponent s is significantly larger than the branched polymer Rouse model prediction of 1.33 and that the relaxation exponent u is much smaller than the Rouse prediction of 0.67, are consistent with entanglements retarding the relaxation of the branched molecules. Entanglements are anticipated to occur due to the increased chain overlap for systems in the vulcanization class.

The measured u, s, and t values indicate that the dynamic scaling law $u=t/(s+t)$ is a *universal* feature of polymer gelation. By plotting values of s and u from the literature as functions of N/N_e, we conclude that these exponents are *universal* for systems with $N/N_e<2$, and that they support the branched polymer Rouse model.

Longer chains between branch points ($N/N_e>2$) lead to *nonuniversal* exponent values that systematically change with the number of entanglements between branch points N/N_e in a continuous fashion. There is no apparent second universality class in the large N limit. A possible resolution of the apparent nonuniversal behavior may lie in some sort of exponential function for the N and ε dependence of the longest relaxation time. Molecular theories for the relaxation of branched polymers [56,69] have an exponential character, and our observed apparent power laws may be small sections of a universal exponential function. The observed trends of the rheological exponents as functions of N/N_e are in qualitative agreement with theory [69]. However, more theoretical work is needed to resolve the large quantitative discrepancies between theory and experiment. In particular, future experimenters need to determine $N/N_e=M_x/M_e$ in addition to the molar mass distribution exponent τ and rheological exponents s, t, and u.

ACKNOWLEDGMENTS

An acknowledgment is made to the donors of the Petroleum Research Fund, administered by the American Chemical Society, for support of this research. In addition, C.P.L. thanks Eastman Kodak Company for financial support and hospitality during the completion of his graduate studies. B. Owens and C. A. Harrison assisted with the SEC experiments. The work benefited significantly from technical discussions with Michael Rubinstein (UNC–Chapel Hill), Jay Janzen (Phillips Petroleum), Hyuk Yu (University of Wisconsin), and Jeffrey R. Gillmor (Eastman Kodak), and we thank them for their interest and insight.

[1] D. Stauffer and A. Aharony, *Introduction to Percolation Theory*, 2nd ed. (Taylor and Francis, London, 1992).
[2] P. G. de Gennes, Recherche **72**, 919 (1976).
[3] V. L. Ginzburg, Fiz. Tverd, Tela (Leningrad) **2**, 2031 (1960) [Sov. Phys. Solid State **2**, 1824 (1960)].
[4] P. G. de Gennes, J. Phys. (France) Lett. **38**, L355 (1977).
[5] S. Alexander, in *Physics of Finely Divided Matter*, edited by N. Boccara and M. Daoud (Springer-Verlag, New York, 1985).
[6] M. Daoud, J. Phys. (France) Lett. **40**, L201 (1979).
[7] W. Burchard, Adv. Polym. Sci. **48**, 1 (1983).
[8] M. Gordon and S. B. Ross-Murphy, Pure Appl. Chem. **43**, 1 (1975).
[9] P. J. Flory, J. Am. Chem. Soc. **63**, 3083 (1941).
[10] W. H. Stockmayer, J. Chem. Phys. **11**, 45 (1943).
[11] W. H. Stockmayer, J. Chem. Phys. **12**, 125 (1944).
[12] P. J. Flory, *Principles of Polymer Chemistry* (Cornell University Press, Ithaca, 1953).
[13] B. H. Zimm and W. H. Stockmayer, J. Chem. Phys. **17**, 1301 (1949).
[14] T. A. Vilgis, in *Comprehensive Polymer Science*, edited by G. Allen and J. C. Bevington (Pergamon, New York, 1989).
[15] D. R. Miller and C. W. Macosko, J. Polym. Sci., Part B: Polym. Phys. **25**, 2441 (1987).
[16] D. R. Miller and C. W. Macosko, J. Polym. Sci., Part B: Polym. Phys. **26**, 1 (1988).
[17] Z. Ahmad and R. F. T. Stepto, Colloid Polym. Sci. **258**, 663 (1980).
[18] R. F. T. Stepto, Acta Polym. **39**, 61 (1988).
[19] D. Stauffer, A. Coniglio, and M. Adam, Adv. Polym. Sci. **44**, 103 (1983).
[20] P. G. de Gennes, *Scaling Concepts in Polymer Physics* (Cornell University Press, Ithaca, 1988).
[21] C. P. Lusignan, T. H. Mourey, J. C. Wilson, and R. H. Colby, Phys. Rev. E **52**, 6271 (1995).
[22] C. P. Lusignan, Ph.D. thesis, University of Rochester, 1996.
[23] M. Rubinstein, R. H. Colby, and J. R. Gillmor, in *Space-Time Organization in Macromolecular Fluids*, edited by F. Tanaka, M. Doi, and T. Ohta (Springer-Verlag, Heidelberg, 1989).
[24] R. H. Colby, J. R. Gillmor, and M. Rubinstein, Phys. Rev. E **48**, 3712 (1993).
[25] J Adler, Y. Meir, A. Aharony, and A. B. Harris, Phys. Rev. E **41**, 9183 (1990).
[26] M. Adam, D. Lairez, F. Boué, J. P. Busnel, D. Durand, and T. Nicolai, Phys. Rev. Lett. **67**, 3456 (1991).
[27] F. Schosseler, H. Benoit, Z. Grubistic-Gallot, C. Strazielle, and L. Leibler, Macromolecules **22**, 400 (1989).
[28] H. Ottavi, J. Phys. A **20**, 1015 (1987).
[29] J. Hoshen, D. Stauffer, G. H. Bishop, R. J. Harrison, and G. D. Quinn, J. Phys. A **12**, 1285 (1979).
[30] H. E. Stanley and H. Nakanishi, Phys. Rev. B **22**, 2466 (1980).
[31] M. Daoud, E. Bouchaud, and G. Jannink, Macromolecules **19**, 1955 (1986).
[32] M. E. Cates, J. Phys. (France) **46**, 1059 (1985).
[33] J. E. Martin, D. A. Adolf, and J. P. Wilcoxon, Phys. Rev. A **39**, 1325 (1989).
[34] M. Daoud, J. Phys. A **21**, L973 (1988).
[35] D. Durand, M. Delsanti, M. Adam, and J. M. Luck, Europhys. Lett. **3**, 297 (1987).
[36] H. H. Winter, Prog. Colloid Polym. Sci. **75**, 104 (1987).
[37] F. Devreux, J. P. Boilot, F. Chaput, L. Malier, and M. A. V. Axelos, Phys. Rev. E **47**, 2689 (1993).
[38] D. Adolf and J. E. Martin, Macromolecules **23**, 3700 (1990).
[39] D. Adolf, J. E. Martin, and J. P. Wilcoxon, Macromolecules **23**, 527 (1990).
[40] J. E. Martin and D. Adolf, Annu. Rev. Phys. Chem. **42**, 311 (1991).
[41] M. A. V. Axelos and M. Kolb, Phys. Rev. Lett. **64**, 1457 (1990).
[42] D. F. Hodgson and E. J. Amis, Macromolecules **23**, 2512 (1990).
[43] A. Koike, N. Nemoto, M. Takahashi, and K. Osaki, Polymer **35**, 3005 (1994).
[44] M. Adam, M. Delsanti, and D. Durand, Macromolecules **18**, 2285 (1985).
[45] E. M. Valles and C. W. Macosko, Macromolecules **12**, 521 (1979).
[46] F. Chambon and H. H. Winter, Polym. Bull. (Berlin) **13**, 499 (1985).
[47] F. Chambon and H. H. Winter, J. Rheol. **31**, 683 (1987).
[48] F. Chambon and H. H. Winter, J. Rheol. **30**, 367 (1986).
[49] S. K. Venkataraman and H. H. Winter, Rheol. Acta **29**, 423 (1990).
[50] J. C. Scanlan and H. H. Winter, Macromolecules **24**, 47 (1991).
[51] H. H. Winter and M Mours, Adv. Polym. Sci. **134**, 165 (1997).
[52] M. I. Aranguren and C. W. Macosko, Macromolecules **21**, 2484 (1988).
[53] J. D. Ferry, *Viscoelastic Properties of Polymers*, 3rd ed. (Wiley, New York, 1980).
[54] P. C. Hohenberg and B. I. Halperin, Rev. Mod. Phys. **49**, 435 (1977).
[55] W. W. Graessley, *Advances in Polymer Science* (Springer, New York, 1974), Vol. 16.
[56] M. Doi and S. F. Edwards, *The Theory of Polymer Dynamics* (Oxford University Press, Cambridge, 1986).
[57] M. Daoud and A. Lapp, J. Phys.: Condens. Matter **2**, 4021 (1990).
[58] M. Daoud and A. Coniglio, J. Phys. A **14**, L301 (1981).
[59] J. E. Martin, D. Adolf, and J. P. Wilcoxon, Phys. Rev. Lett. **61**, 2620 (1988).

[60] M. Gordon and J. Torkington, Pure Appl. Chem. **53**, 1461 (1981).
[61] L. J. Fetters, D. J. Lohse, and R. H. Colby, in *Physical Properties of Polymers Handbook*, edited by J. E. Mark (AIP, NY, 1996), p. 335.
[62] T. H. Mourey and S. T. Balke, in *Chromatography of Polymers: Characterization by SEC and FFF*, ACS Symp. Ser. Vol. 521, edited by T. Provder (American Chemical Society, Washington, DC, 1993).
[63] P. Cheung, R. Lew, S. T. Balke, and T. H. Mourey, J. Appl. Polym. Sci. **47**, 1701 (1993).
[64] L. Leibler and F. Schosseler, Phys. Rev. Lett. **55**, 1110 (1985).
[65] E. V. Patton, J. A. Wesson, M. Rubinstein, J. C. Wilson, and L. E. Oppenheimer, Macromolecules **22**, 1946 (1989).
[66] R. H. Colby, M. Rubinstein, J. R. Gillmor, and T. H. Mourey, Macromolecules **25**, 7180 (1992).
[67] D. J. Plazek, J. Polym. Sci., Part A: Gen. Pap. **6**, 621 (1968).
[68] P. G. de Gennes, C. R. Acad. Sci. Paris B **286**, 131 (1978).
[69] M. Rubinstein, S. Zurek, T. C. B. McLeish, and R. C. Ball, J. Phys. (France) **51**, 757 (1990).
[70] S. A. Bidstrup and C. W. Macosko, J. Polym. Sci., Part B: Polym. Phys. **28**, 691 (1990).
[71] M. Gordon and K. R. Roberts, Polymer **20**, 681 (1979).
[72] M. Gordon, T. C. Ward, and R. S. Whitney, in *Polymer Networks*, edited by A. J. Chompff and S. Newman (Plenum, New York, 1971).
[73] M. Takahashi, K. Yokoyama, T. Masuda, and T. Takigawa, J. Chem. Phys. **101**, 798 (1994).
[74] F. Surivet, T. M. Lam, J.-P. Pascault, and Q. T. Pham, Macromolecules **25**, 4309 (1992).
[75] M. L. Huang and J. G. Williams, Macromolecules **27**, 7423 (1994).
[76] L. Matejka, Polym. Bull. (Berlin) **26**, 109 (1991).
[77] A. Ram, Polym. Eng. Sci. **17**, 793 (1977).
[78] M. Antonietti, K. J. Fölsch, H. Sillescu, and T. Pakula, Macromolecules **22**, 2812 (1989).
[79] R. A. Mendelson, W. A. Bowles, and F. L. Finger, J. Polym. Sci., Part A: Gen. Pap. **28**, 105 (1970).
[80] A. Izuka, H. H. Winter, and T. Hashimoto, Macromolecules **27**, 6883 (1994).
[81] A. Izuka, H. H. Winter, and T. Hashimoto, Macromolecules **25**, 2422 (1992).
[82] E. M. Valles, J. M. Carella, H. H. Winter, and M. Baumgaertel, Rheol. Acta **29**, 535 (1990).
[83] R. H. Colby and M. G. Hansen (unpublished).